Cell Reports
Report

Msh2-Msh3 Interferes with Okazaki Fragment Processing to Promote Trinucleotide Repeat Expansions

Athena Kantartzis,[1] Gregory M. Williams,[3] Lata Balakrishnan,[1] Rick L. Roberts,[3] Jennifer A. Surtees,[3,*] and Robert A. Bambara[2,*]
[1]Department of Biochemistry and Biophysics
[2]Department of Microbiology and Immunology
University of Rochester School of Medicine and Dentistry, Rochester, NY 14642, USA
[3]Department of Biochemistry, School of Medicine and Biomedical Sciences, University at Buffalo, Buffalo, NY 14214, USA
*Correspondence: jsurtees@buffalo.edu (J.A.S.), robert_bambara@urmc.rochester.edu (R.A.B.)
http://dx.doi.org/10.1016/j.celrep.2012.06.020

SUMMARY

Trinucleotide repeat (TNR) expansions are the underlying cause of more than 40 neurodegenerative and neuromuscular diseases, including myotonic dystrophy and Huntington's disease. Although genetic evidence points to errors in DNA replication and/or repair as the cause of these diseases, clear molecular mechanisms have not been described. Here, we focused on the role of the mismatch repair complex Msh2-Msh3 in promoting TNR expansions. We demonstrate that Msh2-Msh3 promotes CTG and CAG repeat expansions in vivo in *Saccharomyces cerevisiae.* Furthermore, we provide biochemical evidence that Msh2-Msh3 directly interferes with normal Okazaki fragment processing by flap endonuclease1 (Rad27) and DNA ligase I (Cdc9) in the presence of TNR sequences, thereby producing small, incremental expansion events. We believe that this is the first mechanistic evidence showing the interplay of replication and repair proteins in the expansion of sequences during lagging-strand DNA replication.

INTRODUCTION

Errors in DNA replication are hypothesized to cause trinucleotide repeat (TNR) sequences to expand (McMurray, 2010), specifically during lagging-strand replication (Ireland et al., 2000; Schweitzer and Livingston, 1998). Lagging-strand maturation requires Okazaki fragments to be processed and joined into a continuous strand. DNA polymerase δ (pol δ) is responsible for the extension of Okazaki fragments and initiates their processing by displacing the 5′ end of one fragment while extending the 3′ end of the preceding fragment (Balakrishnan and Bambara, 2011). The newly displaced DNA forms a 5′ flap structure, which is cleaved by flap endonuclease 1 (Rad27) (Bambara et al., 1997; Lieber, 1997). This creates a nick that is subsequently sealed by DNA ligase I (Cdc9) (Balakrishnan and Bambara, 2011).

Genetic studies in yeast suggest that both Rad27 and Cdc9 prevent TNR repeat expansions, as the downregulation of either protein leads to a higher frequency of expansions (Ireland et al., 2000; Schweitzer and Livingston, 1998). The mismatch repair (MMR) complex Msh2-Msh3 has also been implicated in TNR expansion, as the knockdown of either subunit was shown to lead to a decrease in the expansion rate of CTG and CAG repeats in a mouse model for Huntington's disease (Manley et al., 1999; Owen et al., 2005). Similarly, a lower rate of expansion was also observed in *Msh3*-deficient DM1 transgenic mice, a model for myotonic dystrophy type I (Foiry et al., 2006; van den Broek et al., 2002). Eukaryotic MMR is initiated by the recognition of mispaired sequences, resulting in either small loops [1–13 nucleotides (nt) long] or single nucleotide loops and mispairs, by the Msh2-Msh3 or Msh2-Msh6 repair complex, respectively (Kolodner and Marsischky, 1999). Because the main function of the mismatch proteins is to maintain genome integrity, the role of Msh2-Msh3 in promoting repeat expansions has been an area of intense interest in the past few years.

Here we demonstrate that Msh2-Msh3 contributes to CTG and CAG repeat expansion in *Saccharomyces cerevisiae*. We further present mechanistic details of how Msh2-Msh3 can promote TNR expansions by altering the activity of Rad27 and Cdc9 on DNA intermediates formed during Okazaki fragment processing (OFP). These details were revealed by the dynamic nature of the DNA substrates we employed, which, in contrast to those used in previous studies, were free to adopt various TNR structure conformations. Using this unique system, we observed a bias toward incremental TNR expansion in the presence of Msh2-Msh3.

RESULTS AND DISCUSSION

Msh2-Msh3 Contributes to Sequence Expansion in *S. cerevisiae*

Msh2-Msh3 has been implicated in repeat expansions in mice, and since we intended to examine this phenomenon in yeast, we first questioned whether the Msh complex is required for expansions in *S. cerevisiae*. We used a reporter system that was developed to detect lagging-strand expansions in

Table 1. Tract Expansion Rates in MMR Deficient Strains of *S. cerevisiae*

Repeat Tract[a]	Genetic Background[b]	Tract Expansion Rate (95% CI)[c]
$(CAG)_{25}$	WT (n = 109)	1.2×10^{-6} (6.5×10^{-7} to 2.1×10^{-6})
	msh3Δ (n = 89)	2.4×10^{-7} (1.6×10^{-7} to 2.8×10^{-7})
	msh6Δ (n = 87)	2.4×10^{-6} (1.7×10^{-6} to 2.9×10^{-6})
$(CTG)_{25}$	WT (n = 50)	3.0×10^{-5} (2.1×10^{-5} to 7.4×10^{-5})
	msh3Δ (n = 49)	1.0×10^{-6} (2.8×10^{-7} to 2.2×10^{-6})
	msh6Δ (n = 59)	1.5×10^{-4} (9.0×10^{-5} to 2.0×10^{-4})
$(C,A,G)_{25}$	WT (n = 89)	$<1 \times 10^{-8}$
	msh3Δ (n = 90)	$<1 \times 10^{-8}$
	msh6Δ (n = 30)	$<1 \times 10^{-8}$
$(C,T,G)_{25}$	WT (n = 40)	$<1 \times 10^{-8}$
	msh3Δ (n = 90)	$<1 \times 10^{-8}$
	msh6Δ (n = 51)	$<1 \times 10^{-8}$

See also Figure S1.

[a]Sequence of the repeat tract on the lagging daughter strand.

[b]Genetic background affected bona fide expansions (see Supplemental Information). The observed percentages of expansion for each strain were as follows: WT $(CTG)_{25}$ = 100%; WT $(CAG)_{25}$ = 90%; *msh3Δ* $(CTG)_{25}$ = 91%; *msh3Δ* $(CAG)_{25}$ = 63%; *msh6Δ* $(CTG)_{25}$ = 90%; *msh6Δ* $(CAG)_{25}$ = 55%. These were not incorporated into the rate calculations.

[c]Rates determined by the method of the median, as described by Drake (1991); 95% CIs are from tables calculated by Nair (1940) and Dixon and Massey (1969).

S. cerevisiae (Dixon et al., 2004; Miret et al., 1998). The sequence $(CTG)_{25}$, $(CAG)_{25}$, or scrambled $(C,A/T,G)_{25}$ was positioned on the lagging strand, fused to a *URA3* reporter gene (Figure S1). Expansions of five or more repeats cause inactivation of the *URA3* gene and resistance to 5-FOA. Because *msh2Δ* has essentially the same expansion rate as the wild-type (WT) (Miret et al., 1998), we chose to examine the effect of *msh3Δ* and *msh6Δ*, whose gene products interact with Msh2 to form two distinct heterodimeric complexes. Cells harboring an *msh3Δ* mutation showed a significant decrease in expansion rates for both CTG (~10–20-fold) and CAG (~5-fold) sequence repeats on the lagging daughter strand as compared with the WT strain (Table 1; $p < 0.0001$ for each). This result is specific for the Msh2-Msh3 complex, because *msh6Δ* cells showed a significant increase rather than a decrease in expansion rate, at least for the CTG repeat (~5-fold; Table 1; $p = 0.0091$). Furthermore, the scrambled sequences did not show any significant difference in expansion rate between the WT and mutant strains. These data suggest that the absence of an expansion phenotype in *msh2Δ* cells could derive from opposing effects of Msh2-Msh3 and Msh2-Msh6 on lagging-strand synthesis. Our results show that in similarity to the case with mice, Msh2-Msh3 promotes TNR expansions in *S. cerevisiae*, solidifying the yeast system as a relevant model for characterizing the mechanism of expansion.

The Msh Complex Interferes with Rad27 and Cdc9 Activity on their Cognate Substrates

Msh2-Msh3 has affinity for DNA substrates containing double-strand (ds)/single-strand (ss) junctions. Specifically, Msh2-Msh3 has a preference for binding junctions with 3′ ssDNA, consistent with its role in MMR and double-strand break repair, and also binds 5′ flap intermediates that form during OFP (Surtees and Alani, 2006). To determine whether Msh2-Msh3 binds preferentially to the base of a 5′ flap, we performed 1,10-phenanthroline-copper (OP-Cu) footprinting on duplex DNA containing an 18 nt unannealed region, simulating an 18 nt, 5′ flap intermediate. Msh2-Msh3 bound to the base of a 5′ flap (Figure 1A and Figure S2), with a pattern that is similar to that observed with the 3′ flap (Surtees and Alani, 2006). This is also the site that Rad27 initially binds before cleavage (Gloor et al., 2010; Tsutakawa et al., 2011). To determine whether Msh2-Msh3 can influence Rad27 flap processing, we performed cleavage assays using 5′ flap substrates with varying flap lengths. A titration of Msh2-Msh3 in the presence of Rad27 resulted in a significant decrease (3- to 5-fold) of cleavage products for all flap lengths tested (Figure 1B). To verify the binding specificities of Rad27 and Msh2-Msh3 on a 5′ flap substrate, we performed gel shift assays using a 10 nt and 20 nt flap substrate. After prebinding Rad27 to the substrates (Figure 1C, lanes 2 and 9), we titrated Msh2-Msh3 into the reactions (Figure 1C, lanes 3–7 and 10–14). Msh2-Msh3 competed with Rad27 for binding to flap substrates, as indicated by the disappearance of the Rad27-bound band upon titration of Msh2-Msh3. In combination with the footprinting data, the cleavage and gel shift assay results suggest that Msh2-Msh3 can inhibit Rad27 flap processing by competing for binding to the base of a 5′ flap intermediate (Figure 1B).

Another preferred structure for Msh2-Msh3 binding is a DNA bubble (Surtees and Alani, 2006), a structure that is known to form during polymerase pausing and subsequent DNA misalignment (Liu and Bambara, 2003). It was previously proposed that the ligation of Okazaki fragments containing such structures can lead to sequence expansion (Wells, 1996). To determine whether the activity of Cdc9 is affected in the presence Msh2-Msh3, we designed substrates containing a 12 nt unannealed bubble in the downstream primer. These substrates also contained a nick at a distance of 2, 4, or 6 nt of complementary DNA from the 5′ end of the bubble. The substrate with the 2 nt annealed region could not be ligated into an expanded product (Figure 1D, lane 2) because DNA breathing can prevent it from forming a stable bubble structure (Liu and Bambara, 2003). Even though the 4 nt and 6 nt substrates were ligated, the latter was ligated more efficiently (Figure 1D, lanes 9 and 16). In the presence of Msh2-Msh3, the ligation efficiency of the 4 nt substrate was reduced (Figure 1D, lanes 10–14). Ligation of the 6 nt substrate was unaffected. OP-Cu footprinting of Msh2-Msh3 bound to a 12 nt bubble substrate revealed that Msh2-Msh3 interacts with and distorts DNA up to 4 nt from the 5′ end of the bubble (Figure 1A and Figure S2). The footprinting analysis correlates with the ligation assay results, because the position of the nick influences Cdc9 activity when it is within

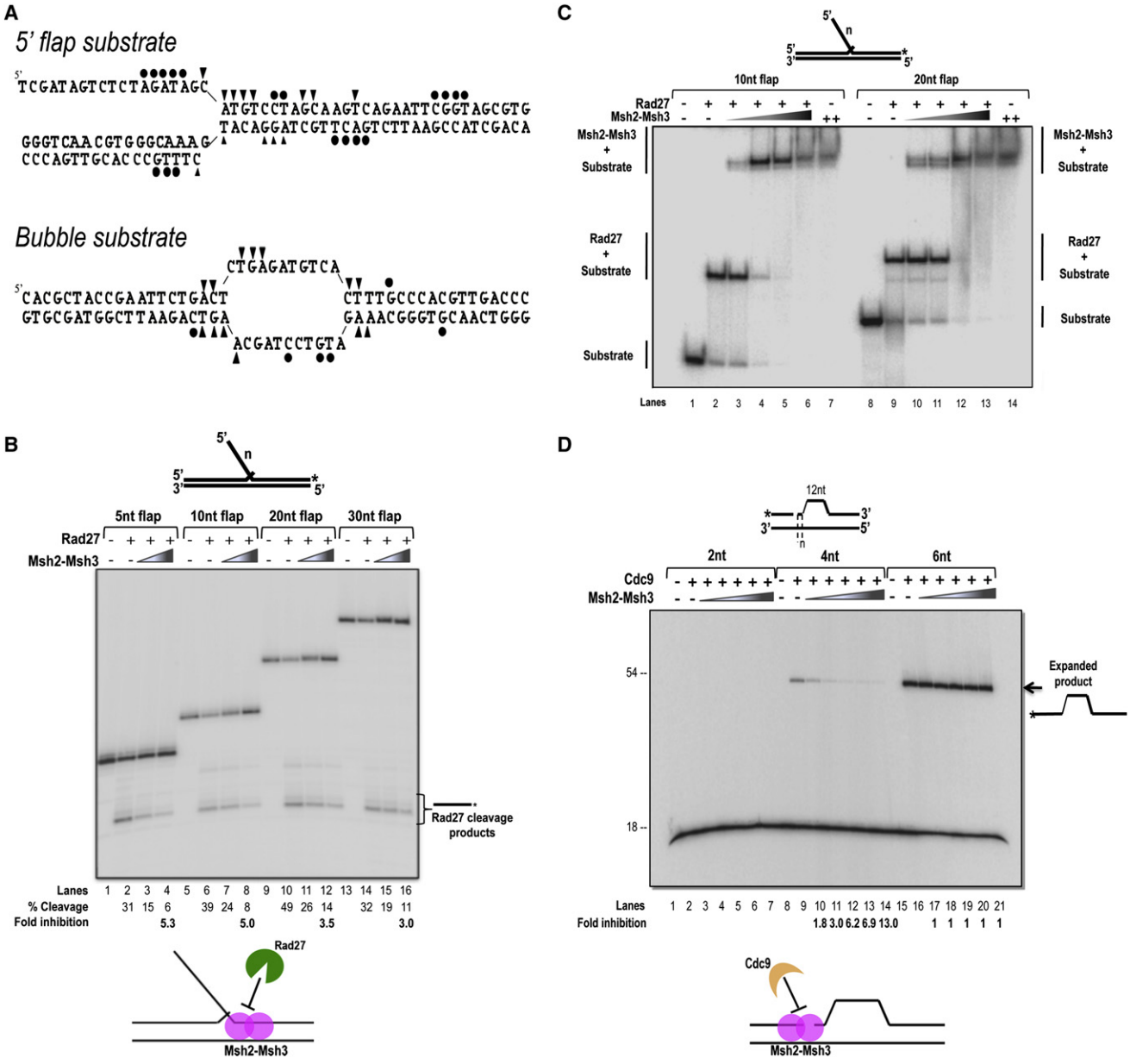

Figure 1. Msh2-Msh3 Interacts with OFP Intermediates to Alter Rad27 Processing and Cdc9 Efficiency

(A) Msh2-Msh3 protection pattern on a 5′ flap substrate (top) and nicked bubble substrate (bottom) resulting from OP-Cu cleavage analysis (see Supplemental Experimental Procedures and Figures S2A and S2B). Circles, protection (<50% of no protein control); triangles, enhanced cleavage (>150% of no protein control).

(B) Rad27 cleavage assay on substrates with various-length 5′ flaps (5, 10, 20, and 30 nt). Substrates were incubated with Rad27 (2.5 nM) and increasing concentrations of Msh2-Msh3 (0, 12.5, and 25 nM). Top: Substrate illustration with asterisk indicating the site of ^{32}P label.

(C) Msh2-Msh3 competes with Rad27 for binding at the base of a 5′ flap. An electrophoresis mobility shift assay was used to study the substrate binding efficiency. Flap substrates (10 and 20 nt) were preincubated with 2.5 nM Rad27 for 10 min before addition of increasing concentrations of Msh2-Msh3 (0, 2.5, 12.5, 25, and 37.5 nM). The labeled substrate is illustrated above, with the asterisk indicating the site of the ^{32}P label. The formed complexes are indicated beside the gel, corresponding to the particular band shift. Bottom: Illustration of Msh2-Msh3 inhibition of Rad27 cleavage.

(D) Ligation assay on substrates containing a 12 nt unannealed bubble region separated from a nick by various-length annealed DNA regions (2, 4, and 6 nt). Substrates were incubated with Cdc9 (12.5 nM) and increasing concentrations of Msh2-Msh3 (0, 2.5, 5, 12.5, 25, and 37.5 nM). Top: Substrate illustration with asterisk indicating the site of ^{32}P label. Bottom: Illustration of Msh2-Msh3 inhibition of Cdc9.

(but not when it is outside of) the Msh2-Msh3 binding region (4 nt or 6 nt, respectively, from the bubble; Figure 1D). Additionally, even though the footprinting data show that Msh2-Msh3 distorts DNA structure, it did not promote the ligation of a DNA bubble into an expanded sequence (Figure 1D, lanes 3–7). Thus, our results suggest that for substrates that cannot be efficiently

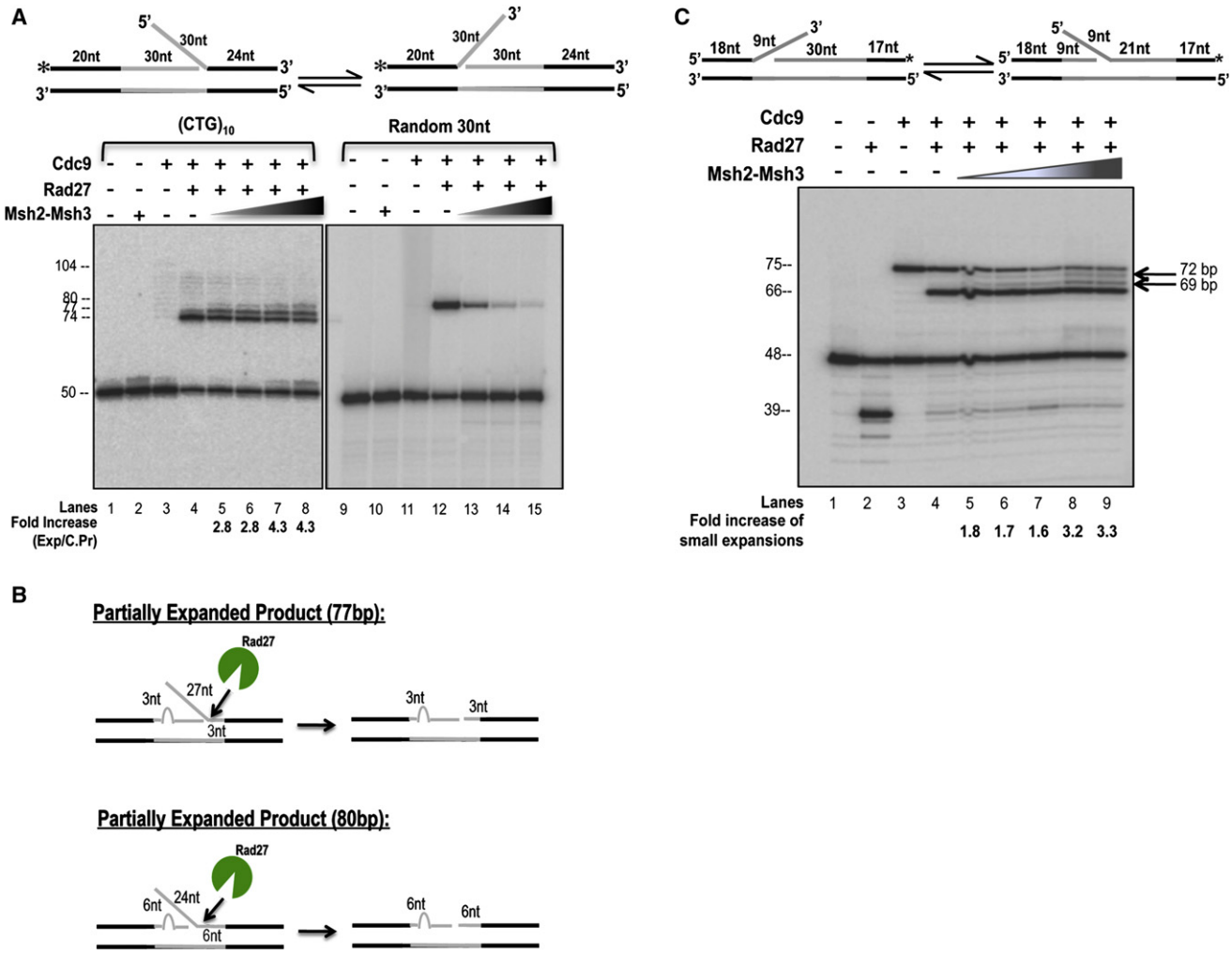

Figure 2. Msh2-Msh3 Interferes with Rad27 Processing and Cdc9 Efficiency to Create Expanded Sequences

(A) Expansion assay on an equilibrating flap substrate, with each flap composed of either 10 CTG repeats or 30 randomly generated nucleotides. Substrates were incubated with Rad27 (2.5 nM), Cdc9 (37.5 nM), and increasing concentrations of Msh2-Msh3 (0, 5, 12.5, 25, 37.5 nM or 0, 12.5, 25, 27.5 nM). Top: Illustration of substrate equilibrating conformations, with asterisk indicating the site of ^{32}P label, and TNRs in gray. See also Figure S3.

(B) Illustration of Rad27 cleavage intermediates for equilibrating flap substrate.

(C) Expansion assay on an equilibrating flap substrate containing equilibrating flaps composed of three CTG repeats. Substrates were incubated with Rad27 (2.5 nM), Cdc9 (37.5 nM), and increasing concentrations of Msh2-Msh3 (2.5, 5, 12.5, 25, 37.5 nM). Top: Illustration of substrate equilibrating conformations, with asterisk indicating the site of ^{32}P label, and TNRs in gray.

ligated (e.g., a 4 nt substrate), Msh2-Msh3 further inhibits their ligation by binding to the nicked sites and blocking Cdc9 activity.

TNR Expansions Are Created by the Coordinated Activity of Rad27, Cdc9, and Msh2-Msh3 during OFP

The presence of Msh2-Msh3 can significantly influence the activity of both Rad27 and Cdc9 on their cognate substrates; therefore, we asked whether it could affect their combined activity on TNR-containing replication intermediates. During replication at TNR tracts, the polymerase has the potential to pause and dissociate from the DNA (Kang et al., 1995; Viguera et al., 2001). Such events allow for the newly synthesized strand and displaced flap to compete for annealing to the template (Liu and Bambara, 2003). To simulate such intermediates, we designed equilibrating flap substrates in which the downstream and upstream primers overlap and compete for template annealing over a 30 nt region. Therefore, the substrate can equilibrate into different conformations, with 5′ and/or 3′ flaps of various sizes, depending on how the primers anneal to the template. The equilibrating sequences consisted of either ten CTG repeats or 30 nt of a randomly generated sequence, which was predicted not to form any structure (Figure 2A). Similarly to previous reports showing that such large flaps cannot be effectively ligated (Veeraraghavan et al., 2003), we did not observe the formation of a fully expanded product (104 bp) in the presence of Cdc9 (Figure 2A, lane 3). Incubation of the substrate with Rad27 and Cdc9 resulted in the majority of products being correctly processed (74 bp; Figure 2A, lane 4), because Rad27 effectively cleaved

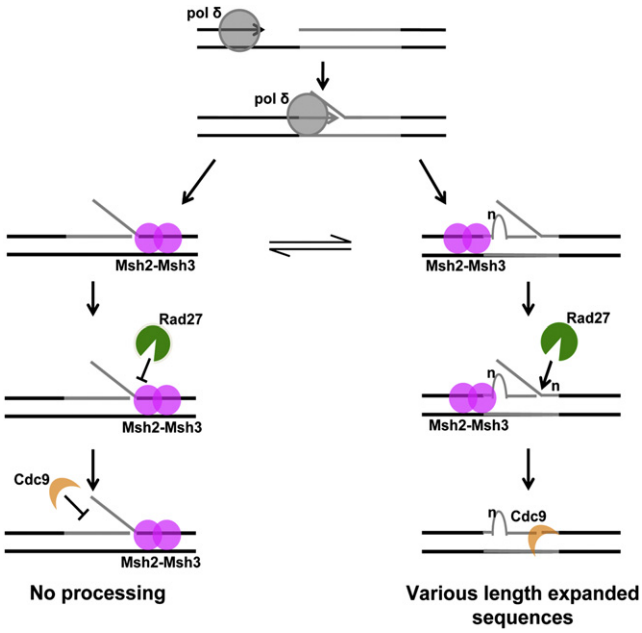

Figure 3. Model of TNR Sequence Expansion in Yeast

During Okazaki fragment maturation, the polymerase (pol δ) reaches the 5′ end of the adjacent Okazaki fragment and causes strand displacement. At TNRs (gray), the polymerase dissociates from the DNA and allows for the newly synthesized strand and displaced 5′ flap to compete for annealing to the template. The DNA equilibrates into multiple structural conformations during this process. Left: The upstream newly synthesized flap anneals completely to the template. Msh2-Msh3 binds at the base of the 5′ flap and inhibits Rad27 and Cdc9. Right: Msh2-Msh3 binds and stabilizes loops of various lengths within the two equilibrating flaps. This causes the 5′ flap to partially anneal to the template and create various-length flaps. Rad27 and Cdc9 process these flaps to create expanded sequences of various lengths.

at the base of the flap, creating a nick for Cdc9 to seal. Of interest, a minority of various-length expansion products was observed only with the substrate containing CTG repeats (Figure 2A, lane 4) and not the randomly generated sequence (Figure 2A, lane 12). Of significance, the titration of Msh2-Msh3 into reactions containing both Rad27 and Cdc9 resulted in the decrease of the correctly processed product and the preferential increase of only smaller expansion products for TNR substrates, corresponding to one or two repeats (Figures 2A, lanes 5–8, and 2B). This increased the ratio of partially expanded to correctly processed products ~4.3-fold as compared with the ratio produced without Msh2-Msh3.

It was previously reported that Rad27 cleavage of such intermediates containing TNRs generates multiple cleavage products because the two competing sequences interact with the template at various positions and equilibrate into different conformations (Liu et al., 2009; Veeraraghavan et al., 2003). This produces various-length 5′ flaps that can be cleaved and ligated to the upstream primer to create expanded products (Figure 2B). To determine whether these expanded products could also be a result of Rad27 cleavage upstream of the flap base, we examined substrates containing only a static 5′ flap consisting of ten CTG, four CTG, or four CAG repeats. Alternate Rad27 cleavage patterns could be observed (Figure S3A), presumably corresponding to secondary structure formation within the 5′ flap (Vallur and Maizels, 2010). Even though Rad27 cleaved at multiple sites upstream of the base (Figure S3A), only a single 2 nt expansion product was observed with the addition of Cdc9 (Figures S3B and S3C), corresponding to a single flap conformation that could be processed into an expanded sequence for this static substrate. Of interest, the presence of Msh2-Msh3 in the reactions promoted the accumulation of the expanded product and decreased the formation of the correctly processed product (Figures S3B and S3C). These results indicate that the cleavage and ligation patterns of TNR-containing 5′ flaps can be altered by the formation of structure within the flap, an effect that is enhanced by the interaction with Msh2-Msh3.

Our findings obtained with a large equilibrating flap indicate that Msh2-Msh3 favors the creation of small expansions rather than large ones. We therefore investigated the effect of Msh2-Msh3 on a smaller equilibrating flap substrate that could efficiently ligate into an expanded sequence. This substrate was designed to contain small equilibrating 9 nt flaps consisting of three CTG repeats that would compete for annealing to the template. Additionally, the downstream primer contained seven more CTG repeats that could fully anneal to the template without competition, in order to enhance the possible structural conformations the substrate could adopt. Incubation with Rad27 resulted in a predominant population of cleavage products that correspond to cleavage at the base of the flap (39 bp; Figure 2C, lane 2). A fully expanded product was also observed upon incubation with Cdc9 (75 bp; Figure 2C, lane 3). The combined addition of Rad27 and Cdc9 produced both a correctly processed (66 bp) and fully expanded product (Figure 2C, lane 4). Upon titration of Msh2-Msh3, however, smaller expansion products (69 and 72 bp) were predominant over the larger fully expanded product (Figure 2C, lanes 5–9). These products are not observed with substrates containing short equilibrating flaps consisting of randomly generated sequences (data not shown). Specifically, Msh2-Msh3 caused up to an ~3.3-fold increase in the accumulation of smaller expansion products (Figure 2C, lane 9). These data are all consistent with Msh2-Msh3 binding and stabilizing small TNR structures that form within the flaps.

Mechanism of TNR Expansion during Lagging-Strand DNA Replication

Our results suggest that Msh2-Msh3 promotes the accumulation of expanded products not only by inhibiting Rad27 cleavage at the base of 5′ flaps but also by stabilizing small loop structures (Lang et al., 2011) formed during the equilibrating conformations of TNR OFP intermediates (Figures 2B and 3). Since our analysis of static TNR 5′ flaps indicated that they are structured, it is likely that a 3′ flap of the same sequence would form structure as well. Thus, it is possible that for equilibrating TNR flaps, the Msh complex not only inhibits the correct processing of 5′ flaps but also binds and stabilizes small loops formed within the 3′ flap, consistent with previous reports showing that Msh2-Msh3 has a binding preference for 3′ flap over 5′ flap intermediates (Surtees and Alani, 2006). This would allow for the downstream 5′ flap to anneal farther along the template and vary in size

(Figures 2D and 3). The cleavage and ligation of such shorter flaps could lead to the creation of an expanded sequence.

Furthermore, our data reveal that the Msh complex also inhibits cleavage of non-TNR flap intermediates. Previous studies suggested that although Msh2-Msh3 can efficiently dissociate from non-TNR DNA structures, it cannot as readily dissociate from TNR structured DNA and remains stuck in a bound conformation (Lang et al., 2011; Owen et al., 2005). Hence, even though we observe Rad27 cleavage inhibition on non-TNR flaps by Msh2-Msh3 in vitro, cellular conditions may regulate the dissociation of the Msh complex from non-TNR repeat structures. The stuck conformation of Msh2-Msh3, however, would allow the protein complex to interfere more effectively with the activity of the replication proteins only on TNR intermediates. Even though Msh2-Msh3 DNA dissociation is dependent on ATP hydrolysis (Gupta et al., 2011; Surtees and Alani, 2006), previous studies showed that it remains stuck on TNR sequences even in the presence of ATP (Lang et al., 2011; Owen et al., 2005). Therefore, we repeated our experiments with ATP. Our results show that expanded products occurred at levels comparable to those reported in Figure 2 (data not shown).

The proposal of a stuck conformation of Msh2-Msh3 bound to TNR structures (Lang et al., 2011; Owen et al., 2005) led investigators to focus on the ability of the complex to initiate or block the repair of these structures. Of interest, studies indicated that Msh2-Msh3 does not interfere with the repair of TNR structures in vitro and can even promote the repair of small loops (Panigrahi et al., 2005, 2010; Tian et al., 2009), which raised questions about the mechanistic role of Msh2-Msh3 in DNA expansion. Those studies, however, were performed in vitro on substrates with a preformed TNR structure. In the study presented here, we instead used equilibrating substrates, which have a propensity to form TNR structures of varying size. Our results obtained with this dynamic system support a model in which Msh2-Msh3 plays a role in TNR expansion by shifting the equilibrium of flaps into many structured conformations, which would affect processing by RAD27 and Cdc9. Even though we observe this effect on equilibrating structures of replication intermediates, it need not necessarily inhibit repair at all TNR structures.

Msh2-Msh3 Promotes Incremental Expansions at TNR Sequences during Lagging-Strand DNA Replication

Our current results indicate a mechanism by which Msh2-Msh3 contributes to short TNR sequence expansions during OFP (Figure 3). Of importance, Msh2-Msh3 promotes short expansions, leading to the incorporation of one or two repeats. We believe that this model for expansion initiation supports the observation that the progression of expansions per replication cycle is very slow (McMurray, 2010). This is in contrast to both nondividing neuronal cells and undifferentiated germ cells, in which expansion events involve the production of longer sequences (McMurray, 2010). Evidently, additional mechanisms can expand TNRs, including errors made during DNA base excision repair (Liu and Wilson, 2012). Additionally, our footprinting analysis of the 5′ flap substrate suggests that Msh2-Msh3 has access to lagging-strand replication intermediates, perhaps to help localize MMR to the lagging strand. Thus, although MMR may be active on both replicating strands, our results suggest that the Msh complex can interact directly with the lagging strand during processing, consistent with reports suggesting that MMR occurs more frequently on this strand (Pavlov et al., 2003). Although the role of Msh2-Msh3 in expansions is counterintuitive, our model suggests that its involvement is an undesirable side-effect of its main function as a repair complex in binding to small loops containing mismatches (Kolodner and Marsischky, 1999). We expect that our findings on the Msh complex role in TNR sequence expansions will contribute to a better mechanistic understanding of how expansions result in neuromuscular diseases.

EXPERIMENTAL PROCEDURES

Protein Expression and Purification

S. cerevisiae Cdc9 (Cdc9p) and Msh2-Msh3 were overexpressed in *S. cerevisiae* and purified as described previously (Ayyagari et al., 2003; Lee et al., 2007; Surtees and Alani, 2006). *S. cerevisiae* Rad27 (Rad27p) was overexpressed in *Escherichia coli* and purified as described previously (Kao et al., 2002).

Fluctuation Analysis

TNR substrates were integrated into WT, *msh3Δ*, and *msh6Δ* strains as described previously (Dixon et al., 2004; Miret et al., 1998). Four different substrates were used and integrated into the three genetic backgrounds, with the following sequence on the lagging daughter strand: (1) a $(CTG)_{25}$ repeat (pBL69), (2) a $(CAG)_{25}$ repeat (pBL70), (3) a scrambled $(C,T,G)_{25}$ repeat (pBL138), and (4) a scrambled $(C,A,G)_{25}$ repeat (pBL139). Each repeat tract was cloned into the regulatory region that controls expression of the *URA3* reporter gene. When the distance between the TATA box and the initiator ATG for the *URA3* gene is increased beyond 29 repeats, *URA3* is no longer expressed, making the cells resistant to 5-FOA. Colonies were then counted and expansion rates calculated as described previously (Drake, 1991). The 95% confidence intervals (CIs) were determined from tables of CIs for the median (Dixon and Massey, 1969; Nair, 1940), and *p* values were determined by Mann-Whitney rank analysis. Also, see Supplemental Experimental Procedures.

Cleavage, Ligation, and Expansion Assays In Vitro

All reactions were performed in 20 μl of 1X MSH buffer (30 mM HEPES, 40 mM KCl, 4 mM $MgCl_2$, 0.01% NP-40, 0.5% inositol, 0.1 mg/ml BSA, 1 mM dithiothreitol [DTT], and 5% glycerol). All reactions were mixed with 0.25 nM DNA substrate on ice and incubated at 37°C for 10 min. Fold inhibition of Rad27 cleavage was calculated by dividing the percentage of Rad27 cleaved in the presence of Msh2-Msh3 by the percentage cleaved in its absence (Balakrishnan et al., 2010). Fold inhibition of Cdc9 activity was calculated by dividing the percentage of Cdc9 ligated in the presence of Msh2-Msh3 by the percentage ligated in its absence (Balakrishnan et al., 2010). Expansions were calculated as the percentage of expanded product divided by the percentage of correctly processed product (Balakrishnan et al., 2010). Fold expansion was calculated by dividing the percentage of expansion in the presence of Msh2-Msh3 by the percentage of expansion in its absence. Also see Supplemental Experimental Procedures.

SUPPLEMENTAL INFORMATION

Supplemental Information includes Extended Experimental Procedures, three figures, and three tables and can be found with this article online at http://dx.doi.org/10.1016/j.celrep.2012.06.020.

LICENSING INFORMATION

ACKNOWLEDGMENTS

We thank Dr. Robert Lahue for the plasmids to generate TNR expansion substrates, Dr. Eric Alani, and Dr. Mark Sutton for a careful reading of the manuscript, Dr. Peter Burgers for sharing purified *S. cerevisiae* DNA ligase I, and members of the Bambara and Surtees laboratories for insightful discussions. This work was supported by National Institutes of Health grants GM098328-01A1 (to L.B.), GM087549 (to J.A.S.), and GM024441 (to R.A.B.).

Received: April 26, 2012
Revised: May 31, 2012
Accepted: June 28, 2012
Published online: August 2, 2012

REFERENCES

Ayyagari, R., Gomes, X.V., Gordenin, D.A., and Burgers, P.M. (2003). Okazaki fragment maturation in yeast. I. Distribution of functions between FEN1 AND DNA2. J. Biol. Chem. *278*, 1618–1625.

Balakrishnan, L., and Bambara, R.A. (2011). Eukaryotic lagging strand DNA replication employs a multi-pathway mechanism that protects genome integrity. J. Biol. Chem. *286*, 6865–6870.

Balakrishnan, L., Gloor, J.W., and Bambara, R.A. (2010). Reconstitution of eukaryotic lagging strand DNA replication. Methods *51*, 347–357.

Bambara, R.A., Murante, R.S., and Henricksen, L.A. (1997). Enzymes and reactions at the eukaryotic DNA replication fork. J. Biol. Chem. *272*, 4647–4650.

Dixon, M.J., Bhattacharyya, S., and Lahue, R.S. (2004). Genetic assays for triplet repeat instability in yeast. Methods Mol. Biol. *277*, 29–45.

Dixon, W., and Massey, F.J.J. (1969). Introduction to Statistical Analysis (New York, USA: McGraw Hill).

Drake, J.W. (1991). A constant rate of spontaneous mutation in DNA-based microbes. Proc. Natl. Acad. Sci. USA *88*, 7160–7164.

Foiry, L., Dong, L., Savouret, C., Hubert, L., te Riele, H., Junien, C., and Gourdon, G. (2006). Msh3 is a limiting factor in the formation of intergenerational CTG expansions in DM1 transgenic mice. Hum. Genet. *119*, 520–526.

Gloor, J.W., Balakrishnan, L., and Bambara, R.A. (2010). Flap endonuclease 1 mechanism analysis indicates flap base binding prior to threading. J. Biol. Chem. *285*, 34922–34931.

Gupta, S., Gellert, M., and Yang, W. (2011). Mechanism of mismatch recognition revealed by human MutSβ bound to unpaired DNA loops. Nat. Struct. Mol. Biol. *19*, 72–78.

Ireland, M.J., Reinke, S.S., and Livingston, D.M. (2000). The impact of lagging strand replication mutations on the stability of CAG repeat tracts in yeast. Genetics *155*, 1657–1665.

Kang, S., Ohshima, K., Shimizu, M., Amirhaeri, S., and Wells, R.D. (1995). Pausing of DNA synthesis in vitro at specific loci in CTG and CGG triplet repeats from human hereditary disease genes. J. Biol. Chem. *270*, 27014–27021.

Kao, H.I., Henricksen, L.A., Liu, Y., and Bambara, R.A. (2002). Cleavage specificity of *Saccharomyces cerevisiae* flap endonuclease 1 suggests a double-flap structure as the cellular substrate. J. Biol. Chem. *277*, 14379–14389.

Kolodner, R.D., and Marsischky, G.T. (1999). Eukaryotic DNA mismatch repair. Curr. Opin. Genet. Dev. *9*, 89–96.

Lang, W.H., Coats, J.E., Majka, J., Hura, G.L., Lin, Y., Rasnik, I., and McMurray, C.T. (2011). Conformational trapping of mismatch recognition complex MSH2/MSH3 on repair-resistant DNA loops. Proc. Natl. Acad. Sci. USA *108*, E837–E844.

Lee, S.D., Surtees, J.A., and Alani, E. (2007). *Saccharomyces cerevisiae* MSH2-MSH3 and MSH2-MSH6 complexes display distinct requirements for DNA binding domain I in mismatch recognition. J. Mol. Biol. *366*, 53–66.

Lieber, M.R. (1997). The FEN-1 family of structure-specific nucleases in eukaryotic DNA replication, recombination and repair. Bioessays *19*, 233–240.

Liu, Y., and Bambara, R.A. (2003). Analysis of human flap endonuclease 1 mutants reveals a mechanism to prevent triplet repeat expansion. J. Biol. Chem. *278*, 13728–13739.

Liu, Y., and Wilson, S.H. (2012). DNA base excision repair: a mechanism of trinucleotide repeat expansion. Trends Biochem. Sci. *37*, 162–172.

Liu, Y., Prasad, R., Beard, W.A., Hou, E.W., Horton, J.K., McMurray, C.T., and Wilson, S.H. (2009). Coordination between polymerase beta and FEN1 can modulate CAG repeat expansion. J. Biol. Chem. *284*, 28352–28366.

Manley, K., Shirley, T.L., Flaherty, L., and Messer, A. (1999). Msh2 deficiency prevents in vivo somatic instability of the CAG repeat in Huntington disease transgenic mice. Nat. Genet. *23*, 471–473.

McMurray, C.T. (2010). Mechanisms of trinucleotide repeat instability during human development. Nat. Rev. Genet. *11*, 786–799.

Miret, J.J., Pessoa-Brandão, L., and Lahue, R.S. (1998). Orientation-dependent and sequence-specific expansions of CTG/CAG trinucleotide repeats in *Saccharomyces cerevisiae*. Proc. Natl. Acad. Sci. USA *95*, 12438–12443.

Nair, K. (1940). Table of confidence interval for the median samples from any continuous population. Sankhya. Ind. J. Stat. *4*, 551–558.

Owen, B.A., Yang, Z., Lai, M., Gajec, M., Badger, J.D., 2nd, Hayes, J.J., Edelmann, W., Kucherlapati, R., Wilson, T.M., and McMurray, C.T. (2005). (CAG)(n)-hairpin DNA binds to Msh2-Msh3 and changes properties of mismatch recognition. Nat. Struct. Mol. Biol. *12*, 663–670.

Panigrahi, G.B., Lau, R., Montgomery, S.E., Leonard, M.R., and Pearson, C.E. (2005). Slipped (CTG)*(CAG) repeats can be correctly repaired, escape repair or undergo error-prone repair. Nat. Struct. Mol. Biol. *12*, 654–662.

Panigrahi, G.B., Slean, M.M., Simard, J.P., Gileadi, O., and Pearson, C.E. (2010). Isolated short CTG/CAG DNA slip-outs are repaired efficiently by hMutSbeta, but clustered slip-outs are poorly repaired. Proc. Natl. Acad. Sci. USA *107*, 12593–12598.

Pavlov, Y.I., Mian, I.M., and Kunkel, T.A. (2003). Evidence for preferential mismatch repair of lagging strand DNA replication errors in yeast. Curr. Biol. *13*, 744–748.

Schweitzer, J.K., and Livingston, D.M. (1998). Expansions of CAG repeat tracts are frequent in a yeast mutant defective in Okazaki fragment maturation. Hum. Mol. Genet. *7*, 69–74.

Surtees, J.A., and Alani, E. (2006). Mismatch repair factor MSH2-MSH3 binds and alters the conformation of branched DNA structures predicted to form during genetic recombination. J. Mol. Biol. *360*, 523–536.

Tian, L., Hou, C., Tian, K., Holcomb, N.C., Gu, L., and Li, G.M. (2009). Mismatch recognition protein MutSbeta does not hijack (CAG)n hairpin repair in vitro. J. Biol. Chem. *284*, 20452–20456.

Tsutakawa, S.E., Classen, S., Chapados, B.R., Arvai, A.S., Finger, L.D., Guenther, G., Tomlinson, C.G., Thompson, P., Sarker, A.H., Shen, B., et al. (2011). Human flap endonuclease structures, DNA double-base flipping, and a unified understanding of the FEN1 superfamily. Cell *145*, 198–211.

Vallur, A.C., and Maizels, N. (2010). Complementary roles for exonuclease 1 and Flap endonuclease 1 in maintenance of triplet repeats. J. Biol. Chem. *285*, 28514–28519.

van den Broek, W.J., Nelen, M.R., Wansink, D.G., Coerwinkel, M.M., te Riele, H., Groenen, P.J., and Wieringa, B. (2002). Somatic expansion behaviour of the (CTG)n repeat in myotonic dystrophy knock-in mice is differentially affected by Msh3 and Msh6 mismatch-repair proteins. Hum. Mol. Genet. *11*, 191–198.

Veeraraghavan, J., Rossi, M.L., and Bambara, R.A. (2003). Analysis of DNA replication intermediates suggests mechanisms of repeat sequence expansion. J. Biol. Chem. *278*, 42854–42866.

Viguera, E., Canceill, D., and Ehrlich, S.D. (2001). Replication slippage involves DNA polymerase pausing and dissociation. EMBO J. *20*, 2587–2595.

Wells, R.D. (1996). Molecular basis of genetic instability of triplet repeats. J. Biol. Chem. *271*, 2875–2878.